

# The anisosphere model: a novel differential phase space representation for Foucault pendulums and 2D oscillators

R Verreault<sup>1</sup>

Université du Québec à Chicoutimi,  
555, boulevard de l'Université, Saguenay, Québec, Canada G7H 2B1.

E-mail: [rverreau@uqac.ca](mailto:rverreau@uqac.ca)

**Abstract.** It is customary to describe the behaviour and stability of oscillators with the help of phase space representation. However, two-dimensional (2D) oscillators like the Foucault pendulum call for a 4D phase space that is not simple to visualize. Applying celestial body perturbation theory to the Foucault pendulum in his doctor dissertation, Nobel laureate Kamerlingh Onnes showed that the essential features of a Foucault pendulum are its inherent circular and linear anisotropies. A spherical differential 2D subspace can be defined, where the group of the points of a spherical surface with respect to the operation *rotation about a diametral axis* is isomorphic with the group of sequential states of oscillation of a 2D pendulum with respect to the operation *translation in time*. Any Foucault pendulum is then characterized by two elliptical eigenstates which are represented by the poles of that rotation axis on the so-called anisosphere. Such poles play the role of attractor/repellor when “*dichroic*” damping is present. Moreover, they move drastically within a meridian plane when nonlinear restoring torque giving rise to Airy precession occurs. The concept of anisosphere constitutes a very powerful tool for analysing and optimizing actual Foucault pendulum implementations. That feature is illustrated by a numerical model.

## 1. Introduction

Textbooks and research articles usually represent the behaviour and stability features of one-dimensional (1D) pendulums with the help of  $\theta-\dot{\theta}$  phase space [1,2]. For n-multidimensional systems like double pendulums or synchronizing Huyghens clocks, a subspace of the 2D or 2nD phase space must be chosen for graphical representations. A typical example of such a subspace is the Poincare map [3] representation. In spite of its apparent simplicity, a Foucault pendulum is a very sophisticated compound pendulum incorporating some flexible parts and for which as many as twelve degrees of freedom have been identified [4]. In its simplest idealization (for instance, Bravais' conical pendulum [5]), a Foucault pendulum in a rotating reference frame can be regarded as a 2D *linear oscillator* (*linear* pertaining here to differential equations) with two non-degenerate circular orbits or eigenstates at slightly different clockwise (cw) and counter clockwise (ccw) rotating velocities with respect to the rotating laboratory frame (*circular anisotropy*, an analogue of circular birefringence or optical activity in optics). According to that model, a rectilinear or planar oscillation resolved into those two circular eigenstates should remain rectilinear and undergo a mere precession of its swinging azimuth. However this model failed to describe real pendulums, which all show a tendency to develop elliptical orbits after a few minutes of operation. Kirchhoff finally addressed the problem by making it the thesis subject of his student Heike Kamerlingh Onnes (KO) [6]. The new essential feature introduced by KO is the unavoidable

<sup>1</sup> To whom any correspondence should be addressed.



variation of swinging frequency as a function of swinging azimuth for rectilinear oscillations (*linear anisotropy*, an analogue of linear birefringence or double refraction in optics). Therefore, in any physical implementation of a Foucault pendulum, simultaneous presence of circular and linear anisotropies must be dealt with, both of which are orthogonal properties in the mathematical sense.

KO's pioneering work was based on the Hamiltonian of the pendulum orbit in the earth gravitational field and on perturbation methods used, until then, exclusively for the orbits of celestial bodies [7]. Since his pendulum incorporated a suspension on crossed knives, he also addressed the problem on uneven wear of the knife edges causing differential damping factors and a corresponding contribution to linear anisotropy. The name *mechanical dichroism* is proposed for that phenomenon, in analogy with dichroism in crystal optics [8]. KO recognized that the output of his mathematical treatment can be illustrated on a sphere, since his formalism involved equations of spherical trigonometry. He could associate each elliptical orbit of the pendulum to a great circle on a sphere, his so-called *characteristic circle*. The evolution of the pendulum ellipses with time was associated with a precession of that great circle on the sphere, as if that great circle would delimitate a disk wobbling on a plane surface. The great circle parallel to this plane surface was named *time circle*. Finally, a third great circle (*lengtecirkel*), freely translated by this author as a *longitude circle* along which the angular measure is twice the swinging azimuth of the major axis of the ellipse, should be taken as the equator of the KO sphere.

However, KO is not very loquacious about his graphical description and its sole figure 2 about the three great circles is not self-explanatory, to say the least. Incidentally, it is only after the concept of anisosphere [9] had been elaborated that this author was in a position, in retrospect, to interpret the KO sphere representation, after realizing that the anisosphere is, in the mathematical sense, a dual of the KO sphere. Indeed, a great circle on the KO sphere corresponds to its two poles (or symmetry axis) on the anisosphere, and vice versa. However, the reverse correspondence from poles to circles has not been exploited by KO, while it is very rich in information on the anisosphere. Some essential features of the anisosphere are recalled in appendix A. In a sense, the anisosphere appears more universal than the KO sphere, for it is also an analogue of the Poincaré sphere [10,11] used in crystal optics for representing the elliptical states of polarized light propagating through anisotropic media. The analogy stands in the fact that the group operation *rotation about a diametral axis* on the Poincaré sphere corresponds to the group operation *translation in space* for elliptically polarized light, while it corresponds to the group operation *translation in time (evolution)* for the pendulum elliptical orbits.

In a previous article [9], the anisosphere concept has been introduced and tested with the help of cases where the linear oscillator approximation can be considered. The most immediate source of dependable experimental data is KO's thesis itself, since his pendulum was operated at amplitudes small enough for the sinusoidal restoring torque to be considered linear. The output of that re-analysis of KO's thesis with the anisosphere is 2-fold:

- despite the very high degree of sophistication of KO's instrument (operation in partial vacuum, adjustable anisotropy in amount and direction, adjustable moments of inertia, remote measurements of azimuths and of minor and major axis amplitudes with the help of a cathetometer), KO mentioned, and the anisosphere confirmed, that his pendulum was very noisy, so that extensive statistical procedures were needed to make sure that his theory was verified at least on the average;
- as in the case of other types of linear oscillators [2,12], very-low-frequency noise predominates (pink noise) in the form of sudden changes in anisotropy parameters, so that within each intermittent anisotropy regime lasting for many tens of minutes, KO's law is obeyed in a deterministic manner with far better accuracy than KO himself could appreciate.

This has established the role of the anisosphere as an efficient graphic solver based on the parametric equations derived by KO for predicting the behaviour of a 2D harmonic oscillator. In this paper, KO's 2-D linear oscillator theory is applied on a differential basis in a scheme of numerical integration. It becomes possible in this way to analyse the behaviour of highly nonlinear pendulums in terms of Airy precession. In a final section, the consequences of angular damping gradient in terms of mechanical dichroism are analysed using some of KO's experiments.

## 2. Foucault pendulum environment

The driving torques acting on a 2D pendulum can be of many different natures. Since the present work deals exclusively with un-sustained pendulums, any torque of magnetic, electrostatic, electrodynamic or electromagnetic nature is ruled out of this analysis. Whenever an influence of such nature is explicitly introduced, its effect can of course be calculated as a perturbation to the basic pendulum. Crane [13] has built a spherical pendulum operating in a magnetic field and Hecht [14] has described it via perturbation theory. Pippard [15] has already addressed an impressive list of perturbing influences that can affect a Foucault pendulum, free running as well as parametrically maintained.

Among the suspension types commonly used for Foucault pendulums, KO [6] used the crossed rocking knives, Allais [16] and Goodey [17,18] used a ball rolling on a plane (paraconical pendulum) and Verreault [19] used the piano-wire-in-chuck suspension or cantilever under traction. Each type of suspension may lead to suspension anisotropy. The rocking knives may rotate about horizontal axes at different heights and with different radii. There are fixed parts in a given azimuth as opposed to rocking parts causing a different moment of inertia at  $90^\circ$  thereof. The paraconical pendulum may roll on a tilted plane or be attached to a twisting beam, not to mention the bob consisting of a vertical disk used by Allais on purpose. An originally curled piano wire under traction generally fails to achieve circular cross-section by a few percent, thus presenting elastic properties, and possibly dissipative motion near the chuck exit, that vary with azimuth. The chuck lack of verticality may also have a small influence.

### 2.1. Ideal Foucault pendulum.

First of all, it must be emphasized that circular anisotropy of the Foucault type does not involve a physical potential well. It is of purely kinematic nature, as a result of inertia with respect to the rotating reference frame of the laboratory. Such an ideal Foucault pendulum undergoes pure precession at a constant rate. The second time derivative of precession angle being zero means that there is no restoring torque in precession. The differential equation for the precession angle  $\dot{\psi} = c_1$  has only a secular solution:

$$\psi = c_1 t + c_2 \quad (c_1, c_2 \text{ constants}).$$

On the anisosphere, the fast eigenstate of an ideal Foucault pendulum in the Northern (or Southern) earth hemisphere is the lower pole  $R$  (or respectively the upper pole  $L$ ). For an initial rectilinear oscillation,  $P_0$  is on the anisosphere equator.  $P(t)$  remains on the equator at all times and the phase circle (see appendix A) is the equator itself. This means that the oscillation remains rectilinear and its azimuth decreases (or increases) steadily. If the initial orbit  $P_0$  is any cw or ccw ellipse, then  $P(t)$  describes a small circle parallel to the equator: the ellipse shape and sense both remain unchanged while the azimuth of the major axis decreases (or increases) steadily at the local Foucault rate. Since a complete cycle of longitude on the anisosphere runs over  $360^\circ$ , the corresponding Foucault period of phase difference is  $360^\circ / (2\dot{\psi}_F)$ , namely the time needed for the pendulum to describe a total precession angle of  $180^\circ$  at the local Foucault rate  $\dot{\psi}_F$ , where  $\dot{\psi}_F$  is typically in degrees per hour. In Groningen, the Foucault period of KO's pendulum is 16.07 h. However, such an ideal Foucault pendulum cannot be realized in practice. All physical Foucault pendulum implementations end up with the concomitant unavoidable presence of a certain amount of linear anisotropy in combination with the Foucault circular anisotropy.

### 2.2. The nature of suspension anisotropy

Linear anisotropy originates from the extremal difference in the swinging frequencies for two orthogonal swinging azimuths. Apart from the restrictions enumerated at the beginning of this section, the swinging motion of all 2D pendulums is caused, to first order, by the vertical component of the terrestrial apparent gravitational acceleration. In the low-amplitude linear-oscillator approximation, an ideal Foucault pendulum is assumed to possess a rotation symmetric paraboloidal gravitational potential well. However, for larger amplitudes, the actual spheroidal gravitational potential well must be considered. The paraconical pendulum implementations known to the author make use of rolling balls at least 6 mm in diameter. The gravitational potential well has then the shape of a rotation symmetric trochoidal surface. The corresponding nonlinearity

is slightly more pronounced than that of the sine function for the spheroidal well. The trochoidal gravitational well also applies to the crossed-knives suspension, since no knife can be infinitely sharp. In fact, all knives become dull with time, and generally not at the same rate. Nevertheless, the trochoid of knives is much closer to the spheroid than the trochoid of rolling balls.

In so far as the piano-wire-in-chuck suspension is concerned, the flexion of the wire at the chuck exit contributes an elastic restoring torque whose effects are added over those of the gravitational torque. For long pendulums, the elastic potential energy may be considered negligible against the gravitational one, but for short pendulums, the elastic influence should be accounted for. In practice, the gradual flexion near the chuck exit results in a shorter effective pendulum length by typically  $\sim 3$  mm for a 13 kg mass at the end of a 1 mm dia. wire. In accordance with common practice in coil spring industry, a wire life exceeding 10 million flexions is expected if the bending stress does not exceed 45% of the elastic limit [20]. Note that if the piano wire on the shelf was coiled tightly, straightening it may result in an elliptical cross-section and in significant suspension anisotropy [21].

Considering that linear anisotropy due to suspension asymmetry results in slightly different effective pendulum lengths for two orthogonal azimuths, and that the effective length for a given azimuth is the radius of curvature of the potential well cross-section containing that azimuth, linear anisotropy must be associated with a slight hyperboloidal deformation of the pre-existing rotation symmetric gravitational potential well. Consequently, *suspension linear anisotropy must therefore be considered gravitational in nature.*

### 2.3. Bob asymmetry.

If the oscillating mass does not show revolution symmetry about the local vertical when at rest, then a linear anisotropy contribution arises as soon as the oscillation plane differs from one of the symmetry planes of the bob. The rate of phase change between oscillation components respectively along the fast and the slow bob eigenaxes is

$$\dot{\delta} = \omega_X - \omega_Y = \bar{\omega} \frac{(I_Y - I_X)}{2\bar{I}} . \quad (1)$$

$Y$  is the swing azimuth aligned with the bob's largest moment of inertia.

Then, KO precession is initiated at once toward the slow eigenaxis  $Y$ . However, if the spin degree of freedom on the bob is not hindered (contrary to the case of crossed knives suspension), and considering that there is a much smaller moment of inertia attached to the spin degree of freedom than those related to the two swing degrees of freedom, it is the bob that will spin to join the major axis of the ellipse. Once the ellipse major axis and the mobile bob  $Y$  axis coincide, each one of the minor axis value of the ellipse, of the spin velocity and of the opposite precession velocity of the ellipse major axis is maximal (spin-orbit coupling) while the linear anisotropy has momentarily dropped to zero. This dynamic situation goes on past the alignment of anisotropy axis and bob symmetry axis, due to inertia. Then the anisotropy changes sign and increases in the other direction. A reverse KO precession sets in until the azimuth difference between ellipse major axis and bob azimuth of maximum inertia becomes as large as in the initial state, but in a mirror symmetrical position on the other side of the coincidence azimuth. From then on, the reverse tendency brings the pendulum back to the initial situation, thus completing a complete KO cycle of bob spin oscillation.

If the pendulum is free to spin without elastic restoring torque, as for the paraconical pendulum (rolling ball suspension), the above spin-orbit oscillation is governed by a strong local modification of the gravitational potential well. Indeed, the difference in moments of inertia is equivalent to a difference in length of the pendulum for two orthogonal directions, hence to a difference in radius of curvature of the gravitational potential well. Therefore, *the spin-orbit coupling is also of gravitational nature.* This spin-orbit behaviour has already been experimentally observed, and taken advantage of, by Allais [22].

If the suspension is of the piano-wire-in-chuck type, torsion of the wire enables the spin degree of freedom. However, on top of the gravitational restoring torque just described, an additional elastic restoring torque contribution also exists. This will result in a higher spin-orbit coupling potential energy and frequency.

At this point, it may be interesting to note that in absence of bob asymmetry, spin-orbit coupling still exists, due to conservation of angular momentum about the vertical axis. However, in this case, there is no potential well deformation and the solution is secular instead of periodic. For instance, when a paraconical pendulum is launched in a rectilinear azimuth, it is readily subject to the constant rate of cw Foucault precession, in the Northern earth hemisphere. Consequently, a spin at constant velocity in the ccw direction also sets in. This phenomenon has also been nicely illustrated by Allais [23], using a symmetrical spherical bob instead of the vertical disk with which he performed practically all his other experiments between 1954 and 1960.

#### 2.4. The Airy effect.

The Airy effect [24] consists of a type of circular anisotropy arising from the spheroidal shape of the gravitational potential well. Airy first mentions that when the elliptical orbit of the pendulum is almost a circle ( $b \approx a$ ) [25], the orbit major axis undergoes a rotation (precession) in the same sense as angular velocity  $\omega$  of the bob travel along the ellipse, at the particular rate

$$\dot{\psi}_A = \frac{3}{8} \omega \frac{a^2}{l^2} . \quad (2)$$

Later [26], he found out that that formula was not valid for low values of  $b/a$ . He derived the new formula valid for  $b/a \ll 1$  :

$$\dot{\psi}_A = \frac{3}{8} \omega \frac{ab}{l^2} , \quad (3)$$

and he assumed without proof that the latter formula should be valid for every axis ratio, since it merges into the first formula for  $b/a \approx 1$ . In fact, Olsson [27], applying Lindsted-Poincaré perturbation method to a 2D harmonic oscillator as the unperturbed starting system, proved the validity of Airy's formula without any restriction on  $b/a$ . The same result was also obtained by Deakin [28] simply from dimensional analysis and symmetry considerations.

### 3. Modelling the Airy effect

On the anisosphere, circular anisotropy of the Airy type must be represented by an axial vector along the  $RL$  polar axis. Its magnitude is twice the Airy precession rate ( $2\dot{\psi}_A$ ), namely the rate of increase of the phase difference between the fast and the slow circular eigenstates. Since precession direction is in the same sense as bob travel along the ellipse, the Airy anisotropy vector is directed toward the faster lower pole  $R$  for cw ellipses, or toward the faster upper pole  $L$  for ccw ellipses.

In order to figure out the effects of non-linearity of the restoring torque at high amplitude, it is very instructive to start up with KO's original pendulum, which was operated at sufficiently low amplitude to be considered a 2D linear oscillator. Figure A4 shows a sequence of 8 states in the evolution of that pendulum over one complete KO cycle lasting 8.1 h. Note that despite the fact that the  $360^\circ$  Foucault phase cycle has a period  $T_F = 16.07$  h at Groningen, the presence of concomitant linear anisotropy in the amount  $\dot{\delta}$  shortens that phase cycle according to the expression

$$T_{KO} = \frac{2\pi}{\sqrt{\dot{\delta}^2 + (2\dot{\psi}_F)^2}} . \quad (4)$$

In the linear-approximation scheme, the evolution of pendulum states is represented on the anisosphere by a circular phase curve described at constant angular speed in the cw sense about the slow elliptic eigenstate  $N$  as centre. Indeed, the diameter  $MN$  characterizes the total anisotropy (circular plus linear) of the pendulum. The origin of longitudes  $2\psi$  and latitudes  $2\chi$  is taken at the slow rectilinear eigenstate  $Y$ , namely the azimuth of the major axis of the ellipse  $N$ . Figure 1 shows a plot of the phase curve for the 2D linear oscillator as a Lon-Lat graph. Since the centre  $N$  of the phase circle does not coincide with the origin of the plot, there is a strong distortion of this plot compared to the actual shape on the anisosphere. In order to give a truer appreciation of the shape of the phase curve on the anisosphere, it is more appropriate to utilize a stereographic projection of the anisosphere on a plane tangent to the sphere at the origin  $Y$  of longitudes and latitudes.

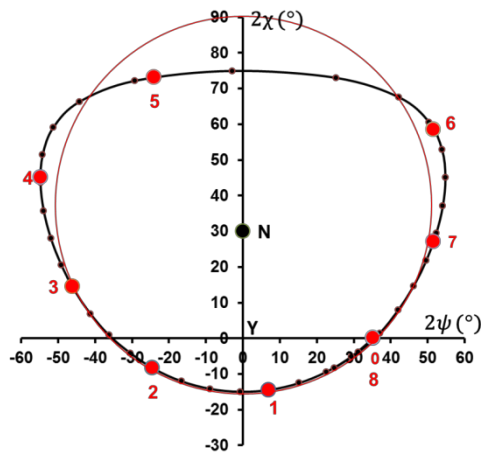


**Figure 1.** Lon-Lat plot of the phase circle for KO's pendulum at 1 mm amplitude (0.0007 rad) on the anisosphere. Since the circle centre *N* does not coincide with the origin *Y*, the phase circle appears distorted on a Lon-Lat plot. The large dots represent the 9 ellipses of the example of KO in figures A3 and A4.

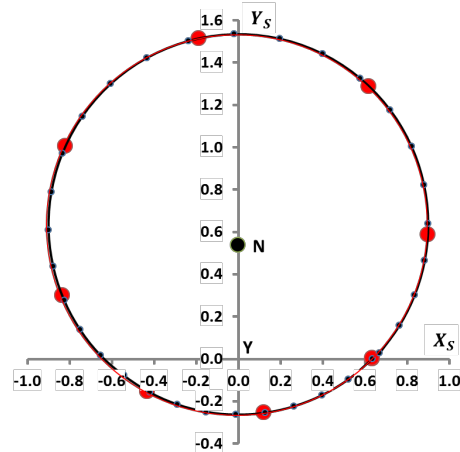


**Figure 2.** Stereographic projection of the phase circle on a plane tangent to the anisosphere at the slow eigenstate *Y*, the projection pole lying at the fast eigenstate *X*. The exact circular shape of the phase curve for the 2D linear oscillator can be appreciated in that type of projection. Amplitude: 0.0007 rad; time step: 900 s; one cycle of precession per 8.1 h.

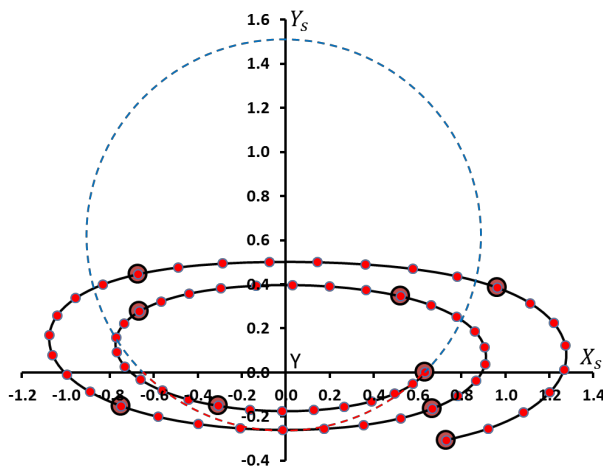


**Figure 3.** Stereographic projection of the phase curve for amplitude 40 mm (0.029 rad). The large dots illustrate how the eight original hourly ellipses of KO have been altered by the nonlinearity of Airy effect. Time step: 455 s; approx. one pseudo-cycle of precession per 4 h.

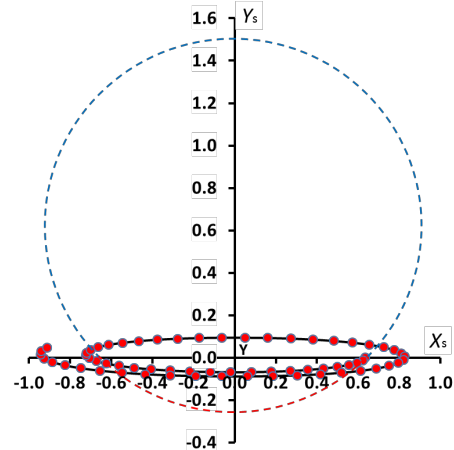


**Figure 4.** Stereographic projection of the phase curve for amplitude 140 mm (0.1 rad). Time step: 100 s; one pseudo-cycle of precession per 1h 18m.

Although the stereographic projection does not preserve distance scales along a given circle arc, it preserves the angles and the shapes locally. In this way, KO theory stating that the phase curve of the 2D linear oscillator should be a circle can easily be verified using the low amplitude case of figure 2. In that figure, the coordinate axes are obtained from the Lon-Lat coordinates  $2\psi$  and  $2\chi$  via the stereographic (subscript *s*) transformation equations

$$X_s = \frac{2 \sin 2\psi \cos 2\chi}{1 + \cos 2\psi \cos 2\chi},$$

$$Y_s = \frac{2 \sin 2\chi}{1 + \cos 2\psi \cos 2\chi}.$$

The reverse transformation is given by

$$2\psi = \sin^{-1} \left( \frac{4X_s}{(4 + X_s^2 + Y_s^2) \cos 2\chi} \right);$$

$$2\psi = \sin^{-1} \left( \frac{4Y_s}{4 + X_s^2 + Y_s^2} \right).$$

Nonlinearity of the Airy type results

- in a collapse of the phase curve onto the anisosphere equator;
- in a shorter phase cycle due to acceleration of precession via the added Airy contribution;
- in an open phase curve spiralling outward from the linear-anisotropy slow eigenstate  $Y$  acting as a repellor.

These features can be observed in figures 3 and 4. Looking more closely at the pendulum's behaviour, it is seen that on starting the pendulum in a rectilinear oscillation (point 0), the initial tangent to the phase curve is the same as in the linear-approximation case, since the initial axis ratio  $/a = 0$ . With the initial azimuth on the positive side of state  $Y$  and with the pivot state  $N$  lying in the upper hemisphere, cw ellipses belonging to the lower hemisphere are first developed. However, as soon as cw ellipses appear, more and more Airy precession rate adds up to the constant Foucault rate. Then the  $MN$  axis changes orientation, within the meridian plane containing states  $X$  and  $Y$ , in such a way that  $M$  approaches  $R$ ,  $N$  approaches  $L$  and  $MN$  becomes more and more parallel to the polar axis  $RL$ . This situation results in a longer radius of curvature for the phase curve as the axis ratio increases negatively, while the total precession rate increases. Therefore, the phase curve is flattened and remains closer to the anisosphere equator than the lower branch (red dotted circle arc below the equator) of the low-amplitude phase circle. Once the phase curve has crossed the equator upwards on the negative azimuth side of state  $Y$ , there is a sudden reversal of precession rate within a few time steps. This happens because, after the slow state azimuth  $Y$  has been crossed, Airy precession rate becomes smaller and smaller until it changes sign by equator crossover of the phase curve and completely compensates the Foucault rate a few time steps later. Then the two eigenstates  $M$  and  $N$  swap hemispheres as the total precession rate also changes sign. As time goes on, eigenstates  $M$  and  $N$  swap hemispheres back again so that a complete cycle of alternating precession rates has been achieved, albeit without repeating exactly the same sequence of ellipticities. Indeed, in the nonlinear case, the phase curve is no longer closed: it rather describes an increasing spiral about the slow linear anisotropy eigenstate  $Y$ . The more nonlinearity there is, the shorter the pseudo cycles of the phase curve. In the examples of figures 2, 3 and 4, the phase cycle (or rather pseudo-cycle) goes from 8.1h for 0.0007 rad amplitude down to  $\sim$ 4h for 0.029 rad amplitude and finally to 1h 18m for 0.1 rad amplitude.

#### 4. Dichroic damping

Anisotropic linear damping is a well-known phenomenon in crystal optics [8, 11]. The mechanical equivalent in pendulums has been observed and calculated via perturbation methods by KO [6]. In optics, the extreme case of dichroism is met with Polaroid filters, as only one of the eigenstates of polarized light gets significantly transmitted by the pellicle of optical material. Similarly, anisotropic damping in a 2D pendulum gradually favours the most lossless eigenstate, which becomes an attractor while the most absorbed state becomes a repellor.

The best illustration of that phenomenon with the anisosphere is obtained from the data of KO's thesis. Since KO was annoyed by his rocking knives becoming dull at different rates, he planned all his significant experiments in pairs, operating once in the azimuthal vicinity of the slow elliptic eigenstate  $N$  and right after, with intentionally the same characteristics of inertial anisotropy, in the azimuthal vicinity of the fast elliptic eigenstate  $M$ , taking the average of the pair in order to eliminate the dichroic effect as much as possible. Figures 5 and 6 show the individual results for such a pair, namely Experiments A-I and A-II of KO's thesis. It is seen that, contrary to strict KO theory according to which the phase curve should be a circular closed curve cw around

the slow elliptic eigenstate  $N$  or ccw around the fast elliptic eigenstate  $M$ , differential damping forces the representative point to describe an outward spiral around the repeller  $N$  and an inward spiral around the attractor  $M$ . Experiments A-I and A-II were each performed over a time span of approximately 3 hours. Assuming that an experiment such as A-II could be pursued without time restrictions, the anisosphere model states that the trace of the pendulum representing point describing the phase curve would spiral around the anisosphere from the slow elliptic eigenstate  $N$  until the fast elliptic eigenstate  $M$ , as would the trace of a knife peeling an apple in one shot from the pedicel all around until the remnants of calyx.

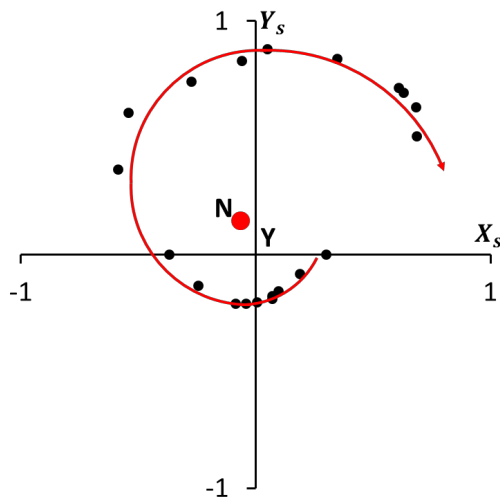


**Figure 5.** Stereographic projection of the phase curve for KO's experiment A-II on a plane tangent to the anisosphere at the equator near the slow elliptic eigenstate  $N$ .

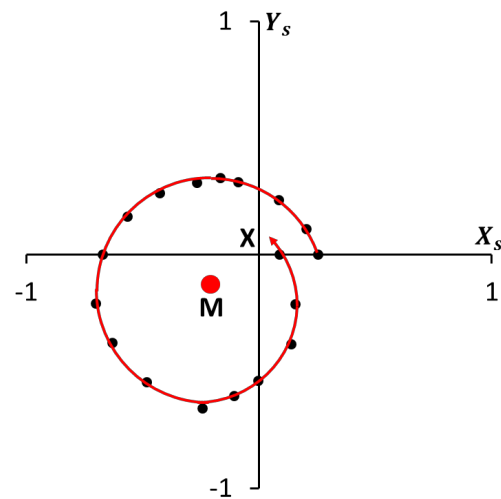


**Figure 6.** Stereographic projection of the phase curve for KO's experiment A-I on a plane tangent to the anisosphere at the equator near the fast elliptic eigenstate  $M$ .

## 5. Discussion

### 5.1. Linear oscillators

In the above sections, the anisosphere model has been applied to a linearly anisotropic Foucault pendulum operating in the Northern earth hemisphere. Any physical implementation of a Foucault pendulum is characterized by the simultaneous presence of circular and linear anisotropy. Linear anisotropy makes things really complicated when quantitative measurements need to be performed with the help of a Foucault pendulum. The anisosphere model enables one to easily visualize the evolution of such a pendulum experiment. In particular, the anisotropy characteristics of said pendulum are very simply described in the form of a diametral rotation axis  $MN$  across the anisosphere model, in such a way that the two surface points  $M$  and  $N$  represent the only elliptical (orthogonal) pendulum oscillations that still remain unaltered with time, the so-called elliptic eigenstates. More generally, any pair of diametrically opposed points on the anisosphere represent orthogonal states. In particular, the diametrically opposed points  $X$  and  $Y$  on the equator at longitudes  $2\psi = 180^\circ$  apart represent respectively the azimuths,  $90^\circ$  apart, of the fastest ( $X$ ) and the slowest ( $Y$ ) rectilinear oscillations of the bob.  $X$  and  $Y$  are at the same time the respective azimuths of the major axes of the eigen-ellipses  $M$  and  $N$ .

It has been shown that at low enough amplitudes, the time sequence of the pendulum oscillation states is represented on the anisosphere model by a small circle centred on the  $MN$  rotation axis. The representing point of the pendulum state actually rotates, as time goes on, along that circle in a cw sense around pendulum's slow elliptic eigenstate  $N$ , or in a ccw sense around the pendulum's fast elliptic eigenstate  $M$ , when looking onto the anisosphere surface from a bird's eye point of



view. If such a low amplitude *linearly anisotropic* pendulum were operated at the earth equator where Foucault circular anisotropy disappears, the anisosphere model allows one to readily visualize what the instrument will do. The  $MN$  rotation axis merges into the  $XY$  diametral axis. All the possible phase circles are in planes normal to the  $XY$  diameter. The duration of the KO cycle would now be given by  $T_{KO} = 2\pi/\dot{\delta}$ . For instance, if the initial rectilinear oscillation has an azimuth  $45^\circ$  higher than the slow state  $Y$ , the initial representative point is at a longitude  $90^\circ$  on the anisosphere equator. The phase circle is then the great circle halfway between states  $Y$  and  $X$  and passing through the anisosphere poles  $R$  and  $L$ . Right from the start, cw ellipses develop for  $\frac{1}{4}$  KO cycle with constant major axis azimuth  $+45^\circ$ , but with steadily decreasing latitude  $2\chi$  until  $2\chi = -90^\circ$ , corresponding to the cw circular orbit. Then there is a sudden discontinuous jump of major axis azimuth from  $+45^\circ$  to  $-45^\circ$  occurs. From then on, major axis azimuth remains  $-45^\circ$  for one  $\frac{1}{2}$  KO cycle while cw ellipses become thinner, merge through a rectilinear state with azimuth  $-45^\circ$  into fatter and fatter ccw ellipses with major axis at  $-45^\circ$  until a ccw circular orbit appears at  $\frac{3}{4}$  KO cycle ( $2\chi = +90^\circ$ ). Then the major axis swaps back to  $+45^\circ$  and ccw ellipses become thinner until the original rectilinear state at  $+45^\circ$  azimuth is reached after one complete KO cycle.

For other starting azimuths at the earth equator, all the phase circles on the anisosphere are small circles normal to the  $XY$  diameter and described in the cw sense about the eigenstate  $Y$  or in the ccw sense about the eigenstate  $X$ , whichever is closer to the initial azimuth. In those cases, no circular orbit is possible. There is some precession of the major axis in such a way that, after  $\frac{1}{4}$  and  $\frac{3}{4}$  KO cycle, the major axis azimuth of the fattest ellipse reached coincides with  $Y$  or  $X$ , whichever is closer to the initial azimuth.

So far, only 2D linear oscillators have been discussed. Incidentally, the anisosphere model can be applied not only to pendulums but to any kind of linear oscillator with two degrees of freedom. This may include two coupled 1D pendulums (Huyghens clocks), wheel suspensions of automobiles, planar triatomic molecules, etc.

### 5.2. Airy effect

It is a well-recognized fact by every serious experimenter with Foucault pendulums that this apparently so simple instrument proves to be very noisy as soon as precision measurements are attempted. A simple glance at every graph in Allais' book [11] is enough to convince anybody. KO himself was obliged to deploy a wealth of imagination in order to attain some reasonable precision in determining the local Foucault precession rate for Groningen. As it can be inferred from figure 5, the scatter of the experimental points was attributed at that time mainly to the uneven wear of the knife edges. However, a recent reanalysis on his data with the anisosphere model [9] has led to the observation that the anisotropy environment aimed at by design was often abruptly modified without control during the course of a typical 3-hour experiment. Fortunately however, KO's precautions to stay clear of perturbing Airy precession have been successful.

On the other hand, with the help of his anisotropic paraconical pendulum, Allais was specifically dedicated at nailing down the anisotropy changes of the pendulum environment. For that purpose, he circumvented the difficulty of measuring very small ellipticity changes by exploiting sensitive Airy precession changes associated with the anisotropy induced ellipticity contributions. In order to correctly interpret his results, it is therefore of the utmost importance to be able to count on a dependable model for the Airy effect in his experiments. The unavoidable reanalysis of his data with the anisosphere model is beyond the scope of this article. However, the ease with which nonlinear Airy precession can be modelled on the anisosphere should help present-day scientists to understand the logic behind his sophisticated experimental procedure, contrary to his contemporary physicists of the French Academy of Sciences who rejected his results from sheer lack of their own scientific knowledge about the pendulum.

The results of figures 3 and 4 are obtained from a mere application of KO's equations during each time step. Notwithstanding the low-frequency noisy character of any pendulum over a finite time lapse, the differential time scale filters out such noise and allows very dependable numerical integration of pendulum motion for analysing nonlinear phenomena. In a companion publication at this Conference, it will be demonstrated by this author how Allais routinely started his experiments on the left side of the phase curve of figures 3 and 4, right at the crossing point of the anisosphere

equator and just before the turning point in precession. His 14-minute long enchainé runs merely covered the part of the phase curve where precession turns about. It will be shown that the final azimuth of such a short experiment is strongly dependent on the azimuthal distance of the slow eigenaxis azimuth  $Y$  on the anisosphere. Allais could in this way monitor the wandering of the slow eigenaxis azimuth in accordance with the position of neighbouring celestial bodies (Moon, Sun ...) during the year.

At the moment of this writing, it is not yet clear whether the fact that the phase curves on figures 3 and 4 are not closed is real or simply an artefact due to the rather coarse time steps of the numerical integration. Unfortunately, time availability did not allow this author to experiment exhaustively with very small time steps before submitting the paper. There is indeed indication from a recent work with an optical analogue of the anisosphere, namely the Poincaré sphere with coordinates in terms of some of the Stokes parameters [11, 29], that the phase curve of Airy precession should be a closed curve with the exact shape of the intersection curve between the sphere and a paraboloidal cylinder. More experimentation is needed on that subject.

However, it must be emphasized that theoretical studies with the Hamiltonian formalism deal strictly with conservative systems. Real pendulums with paraconical suspension involve a third degree of freedom (spin) which interacts with precession but is not represented on the 2D anisosphere surface. It is conceivable that the introduction of spin-orbit coupling in the modelling algorithm of this work would involve borrowing energy from the precession degree of freedom.

## 6. Conclusion

It has been found that the anisosphere model proved very effective and simple in describing the subtle motions of a Foucault pendulum. The evolution of pendulum states in the form of a sequence of elliptical orbits corresponds to simple features on the surface of the anisosphere, namely the representative phase curve. Moreover, the specific anisotropy characteristics of a given pendulum implementation define on the anisosphere a unique diametral rotation axis whose poles represent the elliptical eigenstates (pendulum orbits) which remain unaltered with time. Complex phenomena like angular damping gradient and nonlinear Airy effect can be very simply modelled and visualized with the anisosphere. The novel anisosphere tool makes it now possible to re-analyze highly misunderstood historic experiments. The same tool now enables one to carefully design and analyse future experiments in order to achieve particular measurement goals. The anisosphere model is not just another one of many theoretical approaches that elegantly describe pendulum behaviour. It finds actual practical use as an algorithm to evaluate routine pendulum experiments in quasi-real time and to conduct well planned research programs.

## Acknowledgements

The author is profoundly indebted to Mr Thomas Goodey and Mr Dimitrie Olenici for their dedicated efforts in testing the anisosphere concepts with the help of two exceptional instruments at their Romanian pendularium in Horodnic. Many stimulating discussions with Mr Jean-Bernard Deloly, scientific director of the Fondation Maurice Allais, in Paris, are also gratefully acknowledged.

## Appendix A. Essential features of the anisosphere model

Each oscillation state or orbit of the pendulum bob, as described by figure A1, corresponds to a point  $P$  on the surface of the anisosphere of figure A2. The evolution of the orbit orientation and shape as a function of time results in a particular curve, the *phase curve*, described by the representative point  $P$  on the anisosphere.

The equator of the anisosphere is the locus of the points representing planar pendulum orbits projected as rectilinear oscillations on a horizontal plane, in such a way that the longitude along the equator equals twice the swinging azimuth  $\psi$ ; ( $0 \leq \psi < 180^\circ$ ). Therefore, orthogonal azimuths parallel to the respective axes of a laboratory coordinate system  $XY$  will determine on the anisosphere equator the longitudes of two diametrically opposed points,  $X$  and  $Y$ . The longitude  $2\psi$  is counted positive ccw when looking toward the anisosphere centre from above its upper pole  $L$ .

The latitude  $2\chi$  of point  $P$  is twice the inverse tangent of the minor-to-major axis ratio of the ellipse. Positive latitudes (upper hemisphere) represent ellipses described in the ccw direction by the bob. Then pole  $L$  represents a ccw circular orbit. Similarly, the lower hemisphere represents all the cw ellipses and the lower pole  $R$  represents a cw circular orbit.

Figure A3 is a composite of figures 5 and 6 in KO's thesis where, contrary to the adopted conventions for the anisosphere, the fast and slow eigenaxes are labelled  $y$  and  $x$  respectively. The anisotropy characteristics leading to the 9 orbits of this example have been incorporated into the anisosphere of figure A4. The initial state labelled 0 is rectilinear at an azimuth  $17.5^\circ$  higher than the slow eigenaxis azimuth  $Y$  (or  $x$  in KO's original figure). It is seen that the orbit major axis oscillates about the slow axis, so that orbit 8 finally falls back onto orbit 0.

The parameters of KO's pendulum for pure circular anisotropy are incorporated into figure A4 as axial angular velocity vectors proportional to the rates of increase of the phase difference between the two components of any oscillation resolved along the appropriate eigenstates, namely the ccw ( $L$ ) and cw ( $R$ ) circular orbits. Those for pure linear anisotropy are incorporated as vectors lying in the equatorial plane along the diametral axis  $XY$ . Pure circular (Foucault) anisotropy is represented by the polar vector whose magnitude is the rate of phase change  $2\dot{\rho}$  (twice the Foucault precession rate) and which is pointing toward the faster circular eigenstate  $R$ . Pure linear

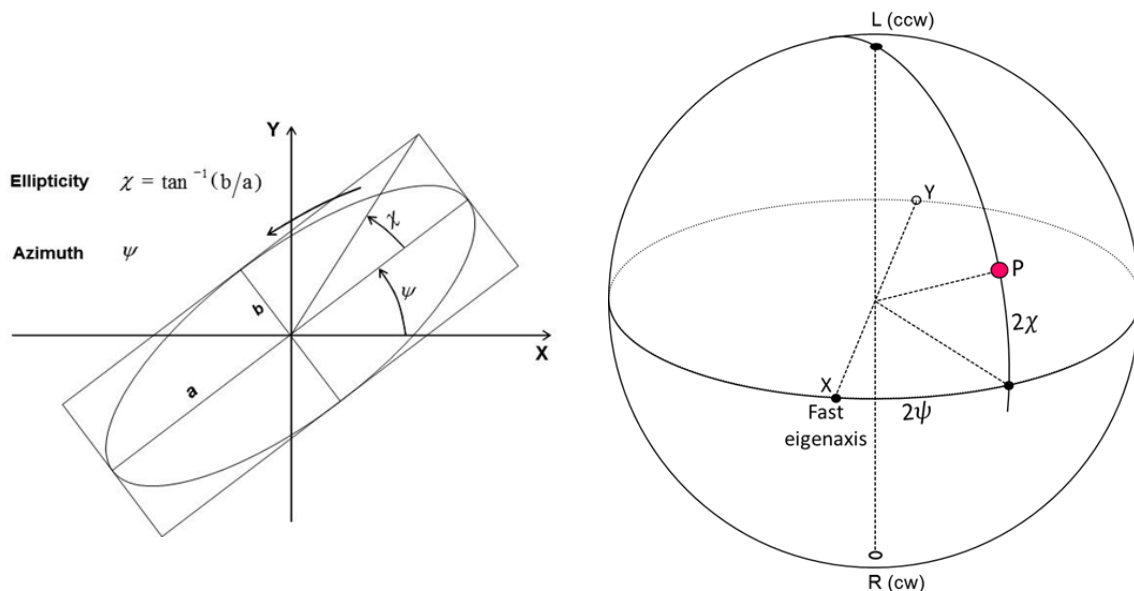


**Figure A1.** Pendulum orbit as seen from suspension point. The parameters of orbit orientation are referred to the linear anisotropy axes.  $X$  represents the fast eigenaxis, namely the azimuth of shortest swinging period.

**Figure A2.** The ccw ellipse of figure A1 is represented by the surface point  $P$  whose longitude is twice the azimuth measured from the fast axis  $X$ , and whose latitude is twice the inverse tangent of the minor-to-major axis ratio.

anisotropy is represented by the equatorial vector whose magnitude is  $\delta = \omega_X - \omega_Y = 2\pi(T_Y - T_X)/T^2$ , and which is pointing toward the faster rectilinear eigenstate  $X$ .

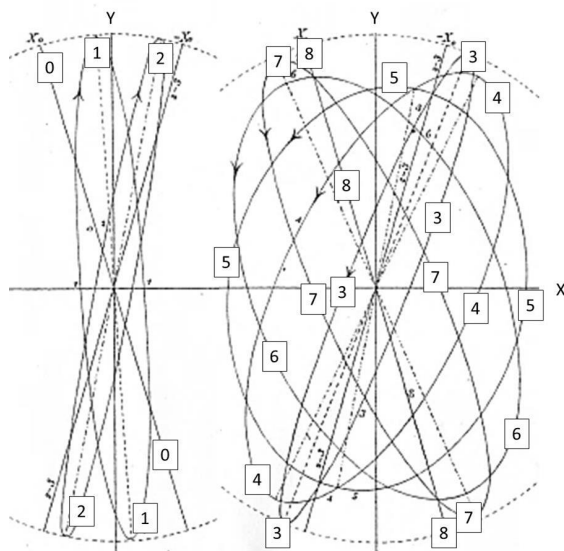
The effect of pure circular anisotropy of the Foucault type in the Northern earth hemisphere is a rotation of the representative point  $P$  about the polar axis in a ccw sense when looking toward the centre from above the faster eigenstate  $R$  (bird's eye view), or a rotation of the representative point  $P$  about the polar axis in a cw sense when looking toward the centre from above the slower eigenstate  $L$ .

The effect of pure linear anisotropy is a ccw rotation of the representative point  $P$  about the equatorial axis  $XY$  when looking toward the centre from above the faster eigenstate  $X$ , or a cw

rotation of the representative point  $P$  about the equatorial axis  $XY$  when looking toward the centre from above the slower eigenstate  $Y$ .

When both types of anisotropy are present, the two angular velocity vectors add up to yield a resultant along a new diametral axis joining the elliptical eigenstates  $N$  and  $M$ , with magnitude  $\dot{\Delta} = [\dot{\delta}^2 + (2\dot{\rho})^2]^{1/2}$  and pointing toward the faster eigenstate  $M$ . The effect of such elliptical anisotropy is a ccw rotation of the representative point  $P$  about the diametral axis  $MN$  when looking toward the centre from above the faster eigenstate  $M$ , or a cw rotation of the representative point  $P$  about the diametral axis  $MN$  when looking toward the centre from above the slower eigenstate  $N$ .

The three situations above strictly apply to the 2D linear oscillator.  $P$  describes then a small circle centred on the diametral axis, the *phase circle*, since the increasing rotation angle is the increasing phase difference between the fast and the slow eigenstates as time runs. It will be shown in further publications that for 2D nonlinear oscillators, the phase curve is no longer a small circle and, in some cases, not a closed curve.



(a) (b)

**Figure A3.** Composite picture from figures 5 and 6 in KO's thesis, with the anisotropy parameter  $\psi' = 30^\circ$  and the initial condition parameter  $\varepsilon = 135^\circ$ . The ellipses have been re-annotated for better legibility. KO's  $x$ -axis was the slow eigenaxis (point  $Y$  on the anisosphere). Linear anisotropy amounts then to  $\sqrt{3}$  times the amount of Foucault circular anisotropy in that example. Note that ellipses 2 and 5 have practically the same azimuth, and the same holds for ellipses 6 and 7. (a) Normal sub-period with cw ellipses and precession in the Foucault sense. (b) Abnormal sub-period with ccw ellipses and precession mostly in the anti-Foucault sense.

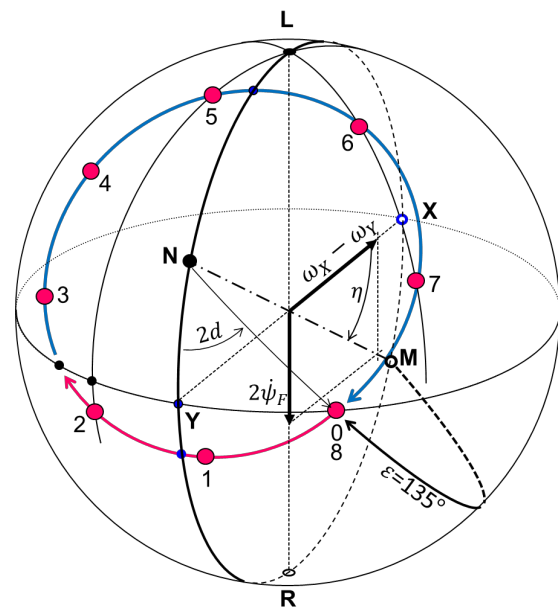


**Figure A4.** Perspective view of the 9 orbits of figure A3 on the anisosphere.  $\varepsilon$  is the great arc distance from fast eigenstate  $M$  to point 0 representing the initial pendulum state. The orbit representative point travels cw at constant angular speed on the phase circle. The radius of the phase circle about the slow eigenstate  $N$  is a great circle arc equal to  $\pi - \varepsilon = 45^\circ$ . In this example, the phase period (or KO period) lasts for 8.03 h and comprises one *normal sub-period* (in red, lower hemisphere), monotonously in the Foucault sense, and one *abnormal sub-period* (in blue, upper hemisphere), where precession is against the Foucault sense for part of its duration.

**References**

- 
- [1] Corinaldesi E 1988 *Classical Mechanics for Physics Graduate Students* (New Jersey: World Scientific)
- [2] Gitterman M 2008 *The Noisy Pendulum* (New Jersey: World Scientific)
- [3] Kapitaniak M, Czolczynski K, Perlikowski P, Stefanski A and Kapitaniak T 2012 *Phys. Reports* **517** 1
- [4] Verreault R 2011 Tidal accelerations and dynamical properties of three degrees-of-freedom pendula *Should the laws of gravitation be reconsidered* ed H A Munera (Montreal: Apeiron) pp 111-126
- [5] Bravais A 1851 *CR* **XXXIII** 195
- [6] Kamerlingh Onnes H 1879 *Nieuwe bewijzen voor de aswenteling der aarde* (Groningen, NL: J B Wolters, also: U. Groningen)
- [7] Schulz-Dubois E O 1970 *Am. J. Phys.* **18** 173-188
- [8] Wahlstrom E E 1969 *Optical crystallography* (New York: Wiley)
- [9] Verreault R 2017 *Eur. Phys. J. Appl. Phys.* **79** 31001 [epjap/2017160337](https://doi.org/10.1051/epjap/2017160337)
- [10] Poincaré H 1892 *Théorie mathématique de la lumière Vol. II Ch. XII* (Paris : Gauthier-Villars)
- [11] Ramachandran G N and Ramaseshan S 1961 *Handbuch der Physik, Bd 5/25* ed S Flüge (Berlin: Springer) pp 1-217
- [12] Chorti A and Brookes M 2006 *IEEE Trans. on Circuits and Systems – I: Regular Papers* **53** 1989-1999
- [13] Crane H R 1981 *Am. J. Phys.* **49** 1004
- [14] Hecht K T 1983 *Am. J. Phys.* **51** 110-114
- [15] Pippard A B 1988 *Proc. Roy. Soc. London A* **420** 81-91
- [16] Allais M 1997 *L'Anisotropie de l'Espace* (Paris: Clément Juglar)
- [17] Goodey T J Pugach A F and Olenici D 2010 *Journal of Advanced Research in Physics* **1**  
Available at:  
<http://stoner.phys.uaic.ro/jarp/index.php?journal=jarp&page=article&op=view&path%5B%5D=20>
- [18] Goodey T J 2011 A Paraconical Odyssey Commences *Should the laws of gravitation be reconsidered?* ed H A Munera (Montreal: Apeiron) pp 231-256
- [19] Verreault R 2007 *Revue Télédétection* **7** 507-524
- [20] Stone R <https://www.mw-ind.com/pdfs/GoodmanFatigueLifeEstimates.pdf>
- [21] Longden A C 1919 *Phys. Rev.* **13**, 241
- [22] Allais M 1997 *L'Anisotropie de l'Espace* (Paris: Clément Juglar), p 243 : note (2); p 246 : insert graphs
- [23] Allais M 1997 *L'Anisotropie de l'Espace* (Paris: Clément Juglar), p 95 : graph IV
- [24] Airy G B 1929 On a means of correcting the length of a pendulum by a ball suspended by wire *Transactions of the Cambridge Philosophical Society* **III** 355-360
- [25] Airy G B 1851 *Proc. Royal Astron. Soc.* **XI** 249-267 On the Regulator of the Clock-work for effective uniform Movement of Equatoreals
- [26] Airy G B 1851 *Proc. Royal Astron. Soc.* **XX** 121-130

- [27] Olsson M G 1978 *Am. J. Phys.* **46** 1119
- [28] Deakin A B 2013 *International Journal of Mathematical Education in Science and Technology* **44** 745-752 DOI:10.1080/0020739X.2012.756550
- [29] Opatrny T and Stepanek P 2018 [arXiv:1806.09485](https://arxiv.org/abs/1806.09485)